Inelastic Scattering of 2.6-Mev Neutrons from Fe^{54}, Fe^{56}, and Fe^{57}

P. SHAPIRO AND R. W. HIGGS
Radiation Division, United States Naval Research Laboratory, Washington, D. C.
(Received July 15, 1957)

Gamma rays following inelastic scattering of 2.6-Mev *d-d* neutrons from isotopically enriched samples of Fe^{54}, Fe^{57}, and from normal iron have been observed in a NaI scintillation spectrometer using the He^3 coincidence technique. The observed gamma rays are listed and are assigned to particular isotopes of the elements studied. Decay schemes are proposed for Fe^{54}, Fe^{56}, and Fe^{57}.

I. INTRODUCTION

OBSERVATION of the gamma rays following inelastic neutron scattering can be used to obtain information on nuclear energy levels. The interpretation of the data from many experiments is complicated by the presence of several isotopes of an element in the scattering sample. Experiments using isotopically enriched scattering samples clarify the isotopic assignment of the observed gamma rays and make it possible to detect previously unobserved gamma rays due to inelastic scattering from the less abundant isotopes.

The He^3 coincidence technique developed at this laboratory[1] makes it possible to use small scattering samples. The reaction $H^2(d,n)He^3$ is used as a neutron source. Scattering events are counted only if they are due to a neutron associated with a He^3 leaving the target within a certain solid angle. Thus the kinematics of the *d-d* reaction can be used to discriminate against those neutrons which do not start out from the target going in the direction of the scatterer. This reduces the effect of the high gamma-ray background due to scattering of neutrons from various materials in the accelerator room.

II. EXPERIMENTAL ARRANGEMENT

The experimental arrangement is indicated schematically in Fig. 1.

Neutrons were produced by bombardment of a thick deuterium target with 250-kev deuterons from a Cockcroft-Walton accelerator. The deuterium target was built up by occlusion of the deuteron beam in an aluminum target backing.

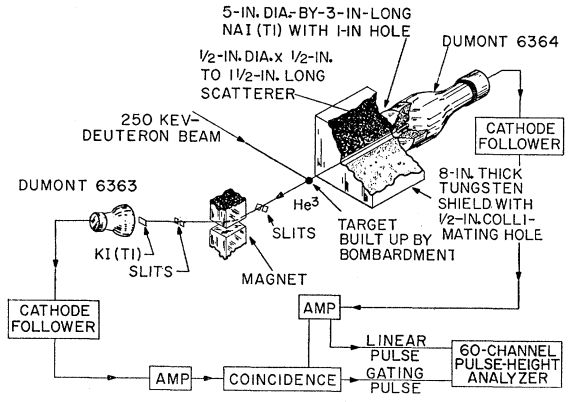

FIG. 1. Schematic arrangement of experimental apparatus.

The 890-kev He^3 particles produced at 76° to the deuteron beam pass through an analyzing magnet and are detected by a bare KI(Tl) scintillation crystal approximately $\frac{1}{16}$ inch thick. The magnetic analyzer was necessary in order to introduce a curved path for the He^3 to traverse from the target to the scintillation crystal. This curved path, light baffles in the vacuum system, and blackening of the interior of the vacuum system prevent light emitted by the target from reaching the scintillation detector. This arrangement was necessary because a light-tight cover over the KI crystal would stop the He^3 particles. The analyzing magnet also helps to separate unwanted charged particles from the He^3 particles. Its resolution was not adequate to completely eliminate deuterons elastically scattered from the aluminum target backing. However, the deuterons can be discriminated against since the KI detector has a higher scintillation response to 890-kev He^3 particles than to the elastically scattered deuterons that get through the magnet.

The 2.6-Mev neutrons at 77° to the deuteron beam, associated with those He^3 selected by the He^3 detector, pass through a $\frac{1}{2}$-inch diameter hole in an eight-inch thick tungsten shield and strike the scatterer. The scatterer is placed inside the well of a NaI(Tl) scintillation detector used as a gamma-ray detector.

The gamma-ray detector is a five-inch diameter by three-inch long NaI(Tl) crystal with a one-inch diameter hole drilled through the crystal along its central axis. This arrangement acts as a summing spectrometer because it has almost 4π geometry and high photopeak efficiency.

The pulse-height distribution from the gamma-ray detector is displayed on a 60-channel pulse-height analyzer. The pulse-height analyzer is gated by the

TABLE I. Isotopic concentration of iron samples.

Isotope	Normal iron	Atomic percent Fe^{54} enriched sample	Fe^{57} enriched sample
Fe^{54}	5.84	94.65	0.226
Fe^{56}	91.68	4.29	56.08
Fe^{57}	2.17	1.02	43.45
Fe^{58}	0.31	0.018	0.244

[1] Faust, Scherrer, and Allison, Phys. Rev. **98**, 224(A) (1955).

signals from the He^3 detector to record only those pulses in coincidence with a He^3.

The scattering samples, $\frac{1}{2}$ inch in diameter, were powdered Fe_2O_3 enclosed in a plastic container. Samples of Fe_2O_3 enriched in Fe^{54} and Fe^{57} were obtained on loan from the Stable Isotopes Research and Production Division of Oak Ridge National Laboratory. The samples used weighed between 3.5 and 5.1 grams. Isotopic concentration of the enriched samples[2] and and that of normal iron are shown in Table I.

III. EXPERIMENTAL PROCEDURE

The current necessary for the analyzing magnet to deflect the He^3 particles into the KI(Tl) crystal detector can be calculated approximately from the known $B\rho$ of the He^3 and the geometry of the analyzing magnet. With this current setting as a starting point, the pulse-height distribution from the He^3 detector was

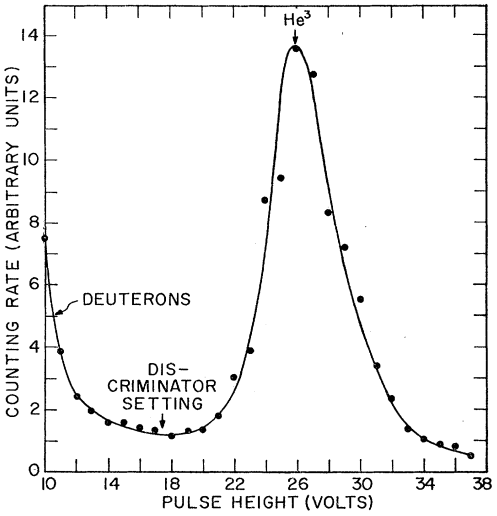

FIG. 2. He^3 pulse-height distribution.

obtained. The magnet current was then adjusted to give maximum counting rate in the He^3 peak. A pulse-height distribution obtained at this current setting is shown in Fig. 2. The He^3 peak is shown accompanied by the lower energy continuous pulse-height distribution from the elastically scattered deuterons. An integral pulse-height discriminator was set as indicated in the figure to discriminate against the deuterons.

The location of the center of the He^3-neutron coincidence beam was determined experimentally by traversing around the expected location with a $\frac{1}{2}$-inch diameter$\times\frac{1}{2}$-inch long stilbene scintillation counter used as a neutron detector. The tungsten shield was then placed with its collimating hole centered at the angle indicated by the maximum coincidence counting rate in the neutron detector. Several times during the

[2] Analysis furnished by Stable Isotopes Research and Production Division, Oak Ridge National Laboratory.

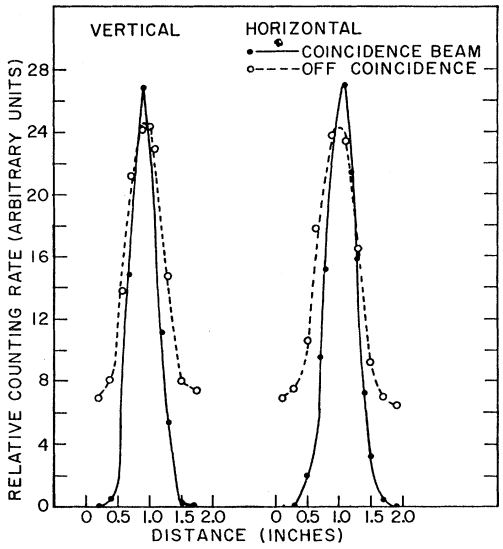

FIG. 3. Traversal of He^3 coincidence beam.

course of these experiments, the coincidence beam was rechecked behind the collimator at the sample location by traversing with the stilbene crystal. A typical coincidence-beam measurement (solid curve) and an off-coincidence transmission curve for the tungsten collimator (dashed curve) are shown in Fig. 3. Ideally, these curves should be centered at the same place. However, repeated measurements of this type indicate that the coincidence beam shifts around by approximately 0.05 inch with respect to the center of the collimating hole.

All runs were taken for a fixed number of singles counts in the He^3 detector which should have been proportional to the number of neutrons in the coincidence beam striking the scatterer. However, various checks on consistency of the data indicate that the He^3 detector is not a good neutron monitor with this arrangement. One source of this difficulty is changes in the location and the focus of the beam spot. This is evidenced by the shifts in the coincidence-beam location previously mentioned. Furthermore, the day-to-day condition of the surface of the deuterium target seems

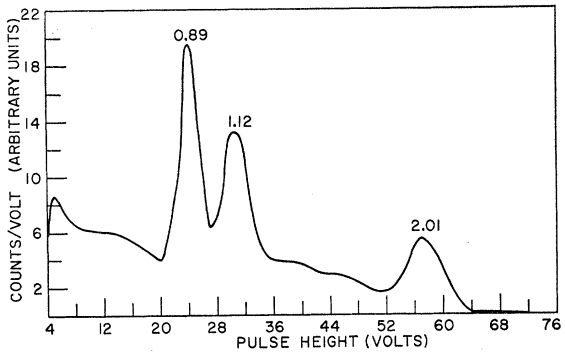

FIG. 4. Pulse-height distribution from Sc^{46}.

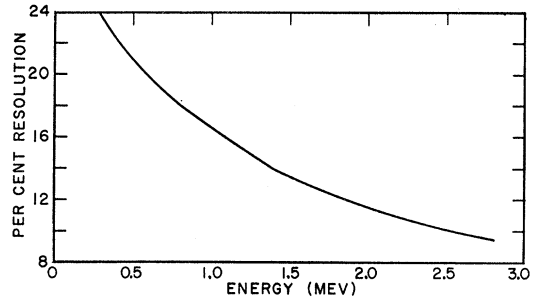

FIG. 5. Percent resolution of gamma-ray spectrometer.

to affect the ability of the He^3 monitor system to distinguish between deuterons and He^3. This is evidenced by changes in the relative height of the He^3 peak to the valley below it. For this reason, no absolute cross sections will be reported here. However, the data on any one scatterer is believed to be consistent with itself since the aforementioned changes occur slowly.

Runs with the scatterer in place were alternated with background runs taken without the sample. The "no sample" runs can be used to subtract off the true-coincidence background.

Another source of background is due to the sample itself. Neutrons scattered elastically from the sample can be scattered inelastically in the NaI crystal, producing gamma rays which are detected in the NaI crystal. These gamma rays, the NaI lines, are then superimposed on the gamma-ray spectrum due to inelastic scattering from the sample. Since the samples are in the form of oxides of the element of interest, neutrons elastically scattered from the oxygen also contribute to the NaI lines. There is no inelastic scattering from oxygen since the first excited state cannot be excited by 2.6-Mev neutrons.[3] Data were taken with a carbon scatterer in order to identify the NaI lines. Since the first excited state of C^{12} is well above 2.6 Mev,[3] there is no inelastic scattering.

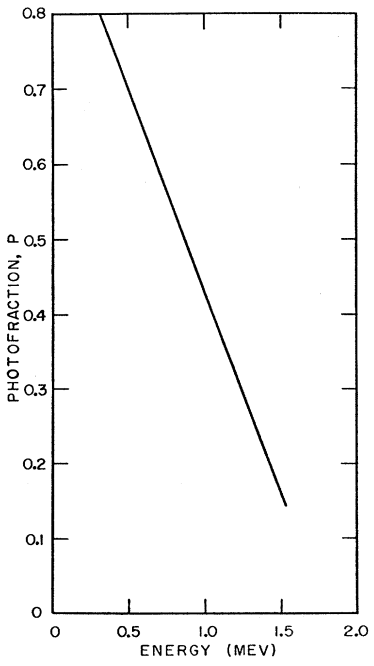

FIG. 6. Photofraction of gamma-ray spectrometer.

IV. GAMMA-RAY SUMMING SPECTROMETER

The summing property of the gamma-ray spectrometer is illustrated by the pulse-height distribution shown in Fig. 4, obtained with a Sc^{46} source placed inside the NaI crystal. Here the photopeaks of the 0.89-Mev and the 1.12-Mev gamma rays[4] and the sum peak at 2.01 Mev are shown.

The photofraction and percent resolution of the gamma-ray spectrometer shown in Figs. 5 and 6, were determined as a function of energy using radioactive sources of monoenergetic gamma rays placed inside the NaI crystal in the same position as the scatterer.

The photopeak efficiency, ϵ, shown in Fig. 7, was determined as follows. The total efficiency, ϵ^T, was

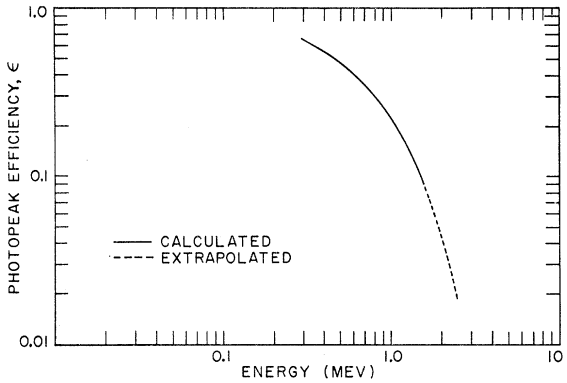

FIG. 7. Photopeak efficiency of gamma-ray spectrometer.

obtained by calculating the probability of a gamma ray interacting in the crystal using the total cross section for NaI with the coherent scattering subtracted.[5] The photopeak efficiency is then obtained from the relation,

$$\epsilon = \epsilon^T P,$$

where P is the experimentally determined photofraction. Since monoenergetic gamma-ray sources were only available up to 1.51 Mev, the photopeak efficiency curve has been extrapolated to obtain ϵ for higher energies.

The analysis of pulse-height distributions from the summing spectrometer to obtain information on the energy levels of the elements under study is discussed

[3] F. Ajzenberg and T. Lauritsen, Revs. Modern Phys. **27**, 77 (1955).
[4] Hollander, Perlman, and Seaborg, Revs. Modern Phys. **25**, 469 (1953).
[5] P. R. Bell, in *Beta- and Gamma-Ray Spectroscopy*, edited by K. Siegbahn (North-Holland Publishing Company, Amsterdam, 1955), p. 153.

elsewhere.[6] The method used is an extension of the work of Gupta and Jha.[7]

V. RESULTS

The pulse-height distributions obtained with the various scatterers are shown in Figs. 8 to 10. The "no sample" background has been subtracted and representative probable errors are indicated. The NaI lines, indicated in Figs. 8 to 10, have been identified from the data shown in Fig. 11 obtained with a carbon scatterer. Gamma rays of energy 0.20, 0.34, 0.43, 0.63, 0.80, 1.00, 1.45, 1.64, and 1.76 Mev are seen. The NaI lines are in reasonable agreement with those observed by other workers,[8] although the summing property of this NaI spectrometer adds extra lines to the spectrum.

When subtracting a photopeak from the pulse-height distribution, one must ascertain the contribution of the NaI lines to the area of the photopeak. One can subtract out the NaI contributions by normalizing the carbon data so that it has the same effect for elastic scattering as the sample of interest. This has been done for the iron data by assuming that the elastic scattering cross section is proportional to the square of the nuclear radius. This method gives reasonable results when applied to the Fe_2O_3 data since the normalized carbon spectrum fits the background between the iron peaks reasonably well except in the neighborhood of the 0.43-Mev NaI line. This discrepancy is believed due to activation of the iodine in the crystal with the emission

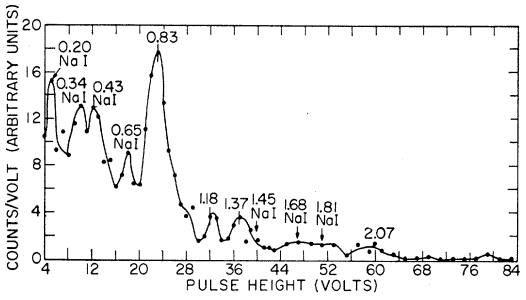

FIG. 8. Pulse-height distribution from normal Fe sample.

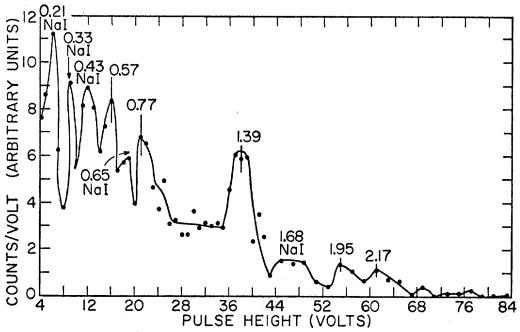

FIG. 9. Pulse-height distribution from enriched Fe^{54} sample.

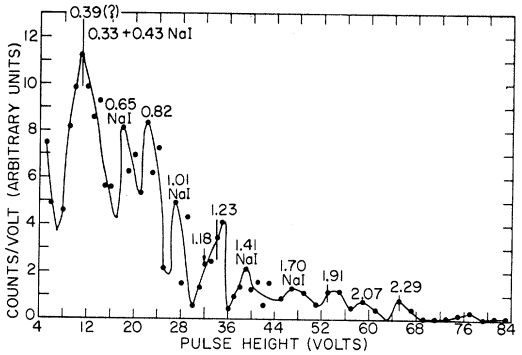

FIG. 10. Pulse-height distribution from enriched Fe^{57} sample.

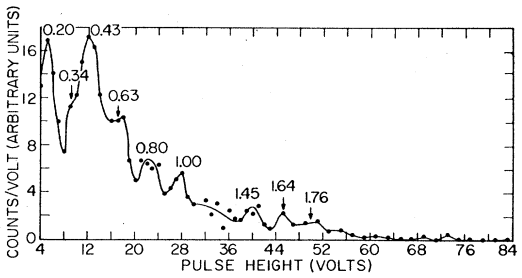

FIG. 11. Pulse-height distribution from carbon sample.

of the 0.428-Mev gamma ray from I^{128} with a 25-minute half-life.[9] This causes the background to depend on the history of the NaI crystal, making it impossible to normalize the yield to the He^3 monitor counts in this region.

The gamma rays observed from the various iron samples are listed in Table II. The energy of the gamma ray is given in Mev, with the isotopic assignment following in parentheses.

Decay schemes are proposed that are consistent with our data. The relative intensity of the various gamma rays has been calculated using the method quoted in Sec. IV. Unfortunately, the counting rate was not high enough to take data with the sample placed in front of the NaI crystal as well as inside it. Lu and Wiedenbeck[10] have shown how comparison of these two types of data will show which gamma rays are in coincidence. This would have provided an additional clue for the interpretation of data.

TABLE II. Gamma ray observed from iron samples.

Normal iron sample	Fe^{54} enriched sample	Fe^{57} enriched sample
0.83±0.03(56)	0.57±0.03(54)	0.39±0.03(57)(?)
1.18±0.03(56)	0.77±0.03(54)	0.82±0.03(56)
1.37±0.03(54)	1.39±0.03(54)	1.18±0.03(56)
2.07±0.05(56)	1.95±0.05(54)	1.23±0.03(57)
	2.17±0.05(54)	1.91±0.05(57)
		2.07±0.05(56)
		2.29±0.05(57)

[6] P. Shapiro and R. W. Higgs, Rev. Sci. Instr. **28**, 939 (1957).
[7] R. K. Gupta and S. Jha, Nuclear Phys. **1**, 2 (1956).
[8] See, for instance, Scherrer, Allison, and Faust, Phys. Rev. **96**, 386 (1954) and R. B. Day, Phys. Rev. **102**, 767 (1956).
[9] Hollander, Perlman, and Seaborg, Revs. Modern Phys. **25**, 546 (1953).
[10] D. C. Lu and M. L. Wiedenbeck, Phys. Rev. **94**, 501 (1954).

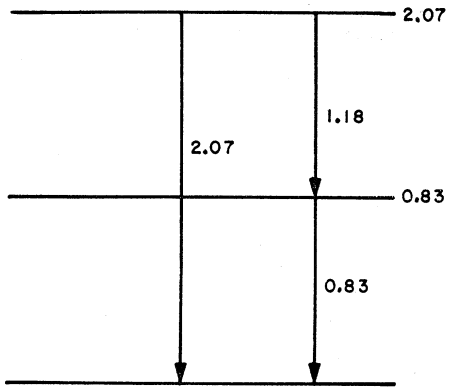

FIG. 12. Decay scheme for Fe^{56}.

Fe^{56}

The gamma rays observed in scattering from normal iron are due mainly to its principal isotope Fe^{56}. Our data are consistent with the well-known energy level scheme of Fe^{56} established from work on the decay of Mn^{56} and Co^{56} and work with nuclear reactions.[11] The decay scheme is shown in Fig. 12. The relative intensity of the various gamma rays has been obtained from our data. Relative intensities have also been computed from other data compiled by Hughes and Carter[12] for inelastic scattering of neutrons of approximately 2.6 Mev. These are compared with our results in Table III. It is to be noted that our work agrees with that of Scherrer *et al.*[13] but is in disagreement with the work of Day.[14]

The 2.07-Mev gamma ray has not been seen by most other workers using neutrons of about 2.6 Mev although it has been observed with higher energy neutrons.[15] Apparently, the photopeak efficiency is not high enough to easily observe this gamma ray with a small NaI crystal.

TABLE III. Relative intensity of Fe^{56} gamma rays.

Gamma-ray energy (Mev)	This experiment	Scherrer[a] *et al.*	Day[b]
0.83	1	1	1
1.18	0.20±0.07	0.17	0.049
2.07	0.30±0.15	...	...

[a] See reference 13.
[b] See reference 14.

[11] Way, King, McGinnis, and van Lieshout, *Nuclear Level Schemes, A=40—A=92*, Atomic Energy Commission Report TID-5300 (U. S. Government Printing Office, Washington, D. C., 1955).
[12] D. J. Hughes and R. S. Carter, "Neutron cross sections, angular distributions," Brookhaven National Laboratory Report BNL-400, June, 1956 (unpublished).
[13] Scherrer, Allison, and Faust (private communication).
[14] R. B. Day, Phys. Rev. **102**, 767 (1956).
[15] See data tabulated in references 11 and 12. An indication of a peak at 2.1 Mev has been reported by Beghian, Hicks, and Milman, Phil. Mag. **46**, 963 (1955) using 2.5-Mev neutrons. However, they are not sure whether it is a sum peak or the photopeak of the 2.1-Mev gamma ray.

TABLE IV. Relative intensity of Fe^{54} gamma rays.

Gamma-ray energy (Mev)	Relative intensity
1.39	1
0.57	0.17±0.08
0.77	0.17±0.08
1.95	0.12±0.06
2.17	0.31±0.16

Fe^{54}

The gamma rays observed from Fe^{54} are listed in Table II. The 1.39-Mev gamma ray has been observed by Sinclair[16] and by Beghian *et al.*[17] in inelastic neutron scattering from enriched Fe^{54} samples. A gamma ray at 2.18 Mev has been observed by Day[14] using a natural iron scatterer. He did not assign this gamma ray to any particular isotope.

Association of the 1.39-Mev gamma ray with the decay of the first excited state is well established from the inelastic proton scattering experiments of Windham *et al.*[18] They observed the first excited state of Fe^{54} at 1.413 Mev by scattering 4.4 to 5.7-Mev protons from enriched Fe^{54} targets. No other levels were observed with an excitation up to 1.6 Mev. Buechner and Sperduto[19] have studied inelastic scattering of 7.04-Mev protons from natural iron. They observed levels in Fe^{54} at 1.41, 2.54, 2.57 Mev, and at higher excitations. Several weaker groups of protons could not be assigned to any particular iron isotope unless isotopically enriched iron targets were used.

After the first excited state is assumed to be at 1.39 Mev, the rest of the decay scheme can be constructed from the energies of the observed gamma rays. The relative intensity of the various gamma rays has been

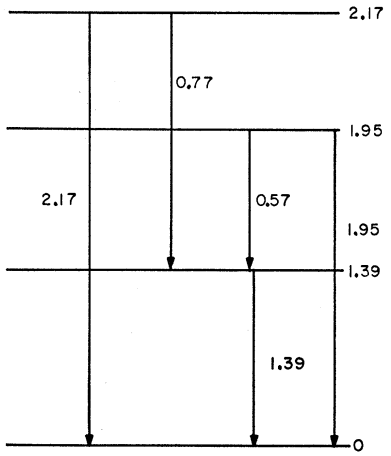

FIG. 13. Proposed decay scheme for Fe^{54}.

[16] R. M. Sinclair, Phys. Rev. **99**, 1351 (1955).
[17] Beghian, Hicks, and Milman, Phil. Mag. **46**, 963 (1955).
[18] Windham, Gossett, Phillips, and Schiffer, Phys. Rev. **103**, 1321 (1956).
[19] W. Buechner and A. Sperduto, Bull. Am. Phys. Soc. Ser. II, **1**, 39 (1956).

calculated and is shown in Table IV. This calculation is based on the decay scheme shown in Fig. 13.

Fe^{57}

The Fe^{57} enriched sample contains almost equal amounts of Fe^{56} and Fe^{57}. However, the gamma rays from Fe^{57} can easily be identified from previous identification of the Fe^{56} gamma rays. Gamma rays of energies 1.23, 1.91, 2.29 Mev, and possibly a 0.39-Mev gamma ray are assigned to Fe^{57}. The presence of a 0.39-Mev gamma ray is indicated by the fact that the 0.33- and 0.43-Mev NaI lines are resolved in the normal iron and the Fe^{54} pulse-height distributions and are not resolved in the Fe^{57} pulse-height distribution.

There is evidence for energy levels in Fe^{57} at 0.014, 0.137, 0.35, 1.27, 1.62, 1.72, and 2.46 Mev and at higher excitations based on work with nuclear reactions and the radioactive decay of Co^{57}. Gamma rays of energies

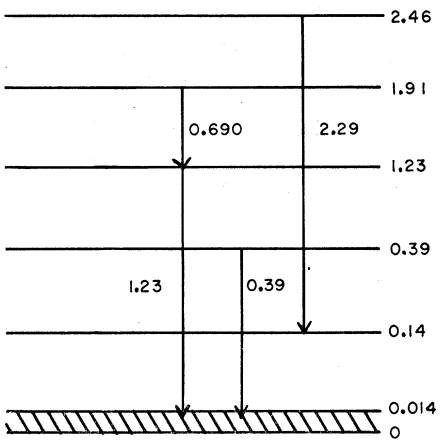

FIG. 14. Proposed decay scheme for Fe^{57}.

0.014, 0.123, and 0.137 Mev, associated with the decay of the 0.014- and 0.137-Mev excited states, have been observed from the decay of Co^{57} and from Coulomb excitation of enriched Fe^{57} targets. In addition to these gamma rays, 0.220, 0.350, and 0.690-Mev gamma rays were observed from the decay of Mn^{57}. The 0.220- and the 0.35-Mev gamma rays are probably associated with the decay of the 0.35-Mev level to the 0.137-Mev level and to the ground state, respectively. The 0.690-Mev gamma ray has not been fitted into the energy level scheme.[11] A 2.3-Mev gamma ray has been seen by Day[14] in the inelastic scattering of 2.56-Mev neutrons from natural iron. This is presumably the same gamma ray observed in this experiment.

A tentative decay scheme is proposed for Fe^{57} and is shown in Fig. 14. This decay scheme was constructed by using clues furnished by this experiment and other available data. It should be noted that no distinction is made between transitions to the ground state and transitions to the 0.014-Mev level as the resolution was such that this distinction could not be made. The gamma ray indicated at 0.39 Mev is assumed to originate from the level previously reported at 0.35 Mev. Since the 2.29-Mev gamma ray has also been observed by Day using a small NaI scintillation detector, this gamma ray is not a sum peak. It is assumed to decay from the previously reported level at 2.46-Mev to the 0.137-Mev level. It is unlikely that a sum peak would be detected since the 0.137-Mev gamma ray is strongly attenuated by self-absorption in the sample. The peak at 1.91 Mev is assumed to be a sum peak, indicating a previously unreported level at 1.91 Mev. This level decays by cascade emission of a 1.23- and a 0.690-Mev gamma ray to the ground state. The 0.690-Mev gamma ray is that observed in the decay of Mn^{57} and was not resolved from the 0.65-Mev NaI line in this experiment.

TABLE V. Relative intensity of Fe^{57} gamma rays.

Gamma-ray energy (Mev)	Relative intensity
0.690	0.72±0.20
1.23	1.00
2.29	1.09±0.55

The possibility was considered that the 2.29-Mev peak is a sum peak indicating an energy level at 2.29 Mev decaying by cascade emission of the 1.91-Mev and the 0.39-Mev gamma rays. This possibility was discarded for the reason discussed in the previous paragraph and because the ratio of the area of the 2.29-Mev peak to the area of the 1.91-Mev peak would have to be much larger than the observed ratio.

The relative intensity of the gamma rays has been calculated assuming the decay scheme shown in Fig. 14, and is shown in Table V.

VI. ACKNOWLEDGMENTS

The authors wish to thank Dr. L. A. Beach, Dr. W. R. Faust, and Dr. C. V. Strain for their active interest and support during the course of these experiments. We would like to thank Mr. A. P. Flanick for his dependable operation of the accelerator, maintenance of the electronic equipment and assistance in taking the data. Messrs. J. L. Warren and G. Lynch were very helpful during their summer employment at NRL. Dr. C. H. Cheek assisted us in preparing the radioactive sources used to calibrate the gamma-ray spectrometer. The enriched isotopes were obtained through the courtesy of the Stable Isotopes Division of Oak Ridge National Laboratory.